doi:10.1093/brain/awaa423

BRAIN
A JOURNAL OF NEUROLOGY

Predictors of volitional motor recovery with epidural stimulation in individuals with chronic spinal cord injury

Samineh Mesbah,[1] Tyler Ball,[2] Claudia Angeli,[1,3,4] Enrico Rejc,[1,2] Nicholas Dietz,[2] Beatrice Ugiliweneza,[1,2] Susan Harkema[1,2,4] and Maxwell Boakye[1,2]

Spinal cord epidural stimulation (scES) has enabled volitional lower extremity movements in individuals with chronic and clinically motor complete spinal cord injury and no clinically detectable brain influence. The aim of this study was to understand whether the individuals' neuroanatomical characteristics or positioning of the scES electrode were important factors influencing the extent of initial recovery of lower limb voluntary movements in those with clinically motor complete paralysis. We hypothesized that there would be significant correlations between the number of joints moved during attempts with scES prior to any training interventions and the amount of cervical cord atrophy above the injury, length of post-traumatic myelomalacia and the amount of volume coverage of lumbosacral enlargement by the stimulation electrode array. The clinical and imaging records of 20 individuals with chronic and clinically motor complete spinal cord injury who underwent scES implantation were reviewed and analysed using MRI and X-ray integration, image segmentation and spinal cord volumetric reconstruction techniques. All individuals that participated in the scES study ($n = 20$) achieved, to some extent, lower extremity voluntary movements post scES implant and prior to any locomotor, voluntary movement or cardiovascular training. The correlation results showed that neither the cross-section area of spinal cord at C3 ($n = 19$, $r = 0.33$, $P = 0.16$) nor the length of severe myelomalacia ($n = 18$, $r = -0.02$, $P = 0.93$) correlated significantly with volitional lower limb movement ability. However, there was a significant, moderate correlation ($n = 20$, $r = 0.59$, $P = 0.006$) between the estimated percentage of the lumbosacral enlargement coverage by the paddle electrode as well as the position of the paddle relative to the maximal lumbosacral enlargement and the conus tip ($n = 20$, $r = 0.50$, $P = 0.026$) with the number of joints moved volitionally. These results suggest that greater coverage of the lumbosacral enlargement by scES may improve motor recovery prior to any training, possibly because of direct modulatory effects on the spinal networks that control lower extremity movements indicating the significant role of motor control at the level of the spinal cord.

1 Kentucky Spinal Cord Injury Research Center, University of Louisville, Louisville, KY, USA
2 Department of Neurosurgery, University of Louisville, Louisville, KY, USA
3 Department of Bioengineering, University of Louisville, Louisville, KY, USA
4 Frazier Rehab Institute, University of Louisville Health, Louisville, KY, USA

Correspondence to: Maxwell Boakye, MD
Kentucky Spinal Cord Research Center
University of Louisville, School of Medicine, 220 Abraham Flexner way, Louisville, KY, USA
E-mail: max.boakye@louisville.edu

Keywords: spinal cord injury; magnetic resonance imaging; spinal cord epidural stimulation; neuromodulation

Abbreviations: AIS = American Spinal Injury Association Impairment Scale; CSA = cross-section area; scES = spinal cord epidural stimulation; SCI = spinal cord injury

Received February 24, 2020. Revised May 25, 2020. Accepted September 30, 2020.

Introduction

Spinal cord injury (SCI) is the second leading cause of paralysis in the USA with over 1.4 million individuals currently living with SCI-related disabilities (Armour *et al.*, 2016). Restoration of voluntary movement, bladder, bowel and sexual function are among top priorities of the SCI population (Anderson, 2004). To date there are no pharmacological treatments that have enabled voluntary movement in those completely paralysed. In previous studies, some individuals that are diagnosed with clinically motor complete injuries have shown motor pool activation below the injury level during volitional attempts (Sherwood *et al.*, 1992; McKay *et al.*, 2004). However, the volitional descending inputs passing through the residual connections alone have not been shown to lead to eliciting movement. Moreover, studies have shown that engaging the sensory feedback via locomotor training interventions were also insufficient to promote sustained recovery of independent standing or stepping in the vast majority of clinically diagnosed motor complete cases (Waters *et al.*, 1992; Wernig *et al.*, 1995).

Spinal cord epidural stimulation (scES) was shown to enable voluntary movement in completely motor paralysed individuals following SCI (Harkema *et al.*, 2011; Angeli *et al.*, 2014). Subsequently, many reports confirmed scES ability to enable voluntary movements and standing and eventually stepping and walking over ground (Grahn *et al.*, 2017; Rejc *et al.*, 2017; Angeli *et al.*, 2018; Gill *et al.*, 2018; Darrow *et al.*, 2019); as well as improved cardiovascular (Aslan *et al.*, 2018; West *et al.*, 2018; Harkema *et al.*, 2018*a*, *b*), and bladder function (Herrity *et al.*, 2018) in the chronic and diagnosed motor complete SCI population who did not have clinically detectable supraspinal influence. Understanding factors that modulate the response to scES is important in designing the best scES strategies to optimize results for the SCI population. This might include implementing strategies that lead to achievement of neuromodulatory goals and improvements in the shortest amount of time using the smaller electrical stimulation intensities.

The device implantation in individuals with chronic SCI currently involves placement of an electrode array at the lumbosacral segment of the spinal cord in a vertebral location typically between the T11 and L1 pedicles (Calvert *et al.*, 2019). The location of the stimulation paddle electrode is guided by intraoperative fluoroscopy and electrophysiology mapping to identify segments of the spinal cord that respond best to electrical stimulation. Following the surgery, additional neurophysiological spatiotemporal mapping of various electrode configurations are used in combination with the motor task (voluntary leg movement, standing or stepping) to restore motor control in individuals with chronic motor complete injuries (Angeli *et al.*, 2014; Rejc *et al.*, 2015).

The evidence of restoration of volitional motor function with scES has suggested that in the presence of scES with appropriate targeted electric fields, the spinal networks of the lumbosacral spinal cord would reach the excitability state needed to interpret the residual volitional descending inputs and sensory information to generate meaningful motor output (Rejc and Angeli, 2019). Spatially and temporally targeting the posterior roots of specific motor pools is another approach to facilitate motor recovery in incomplete SCI (Wagner *et al.*, 2018). There exists considerable variability regarding the extent of individuals' volitional recovery with epidural stimulation and many unidentified factors that influence an individual's response to epidural stimulation.

While almost a decade has elapsed since the initial discovery that scES can restore voluntary movements in paralysed individuals (Harkema *et al.*, 2011), the extents to which the variability of the shape and size of the spinal cord, the severity of the injury and the location of the electrode array with respect to the lumbosacral enlargement and conus medullaris correlate with functional outcomes have not yet been reported. There is considerable heterogeneity in the SCI population that can potentially affect volitional responses with scES including participant's age, duration of injury, type of injury, length of severe myelomalacia, amount of spinal cord atrophy after injury, size of the lumbosacral enlargement, as well as final position of the electrodes in relation to the lumbosacral enlargement of the cord.

In this study, we reviewed MRI, X-rays and clinical records of research participants that have undergone scES implantation at our centre from 2014 to 2019. Our goal in this study was to explore correlations between the amount of cervical cord atrophy above the injury, the length of the injury myelomalacia and the number of joints moved in the presence of scES. Correlations were also examined between number of joints moved and the amount of terminal lumbosacral enlargement coverage, and paddle position with respect to the tip of the conus and maximal cross-section area (CSA) of the lumbosacral enlargement. Our first hypothesis was that individuals with a greater amount of cord atrophy and length of myelomalacia would show a worse volitional movement ability. The second hypothesis was that individuals who had greater coverage of the lumbosacral enlargement by the paddle electrode would exhibit greater number of joints moved. The findings of this study can expand our knowledge and understanding of the mechanisms underlying recovery of volitional movement after severe SCI with scES, as well as help us to understand whether MRI-driven measurements are important predictors of individual responses to scES and guide optimal positioning of the paddle electrode for the best responses.

Materials and methods

Study design

Twenty participants were enrolled in research studies conducted at the University of Louisville investigating the effects of

Table 1 Demographic and clinical characteristics of research participants

Subject id	Gender	At the time of implant				Number of joints moved post implant
		Age (years)	Time since injury (years)	Level of injury	AIS	
A101	Male	31.4	2.4	C3	A	5
A99	Male	19.9	2.8	C4	A	4
A96	Female	26.9	3.1	C4	A	5
A41	Male	24.0	7.2	C4	A	3
A82	Male	36.6	7.4	C4	A	6
A123	Male	29.4	7.8	C4	A	6
A105	Male	33.7	10.0	C4	A	4
A100	Male	52.0	16.6	C4	A	5
A68	Male	35.0	3.8	C5	A	1
A110	Female	22.0	5.8	C5	A	6
A77	Female	28.5	10.2	C5	A	3
A80	Female	32.9	7.9	C6	A	1
A60	Male	23.3	3.2	T3	A	6
A59	Male	26.6	2.5	T4	A	6
B21	Male	31.0	6.9	C4	B	2
B32	Male	60.6	7.4	C4	B	2
B23	Male	32.0	3.3	C5	B	1
B24	Male	25.5	6.7	C6	B	6
B41	Male	26.7	8.6	C8	B	3
B30	Female	22.8	3.2	T1	B	6

activity-based recovery training in combination with scES for lower limb motor function (Rejc *et al.*, 2017) as well as studies investigating the use of scES for the restoration of cardiovascular regulation between 2014 and 2019 (Harkema *et al.*, 2018*b*). All research participants were over 21 years of age at the time of implant with non-progressive SCI above T10, American Spinal Injury Association Impairment Scale (AIS) (Kirshblum *et al.*, 2011) A or B, at least 2 years post-injury, with functional segmental reflexes below the lesion and no clinically detectable brain influence on spinal reflexes. Moreover, none of the participants had any medical conditions unrelated to SCI during the scES implant and training. All research participants provided written informed consent, and the research was approved by the Institutional Review Board (University of Louisville, Louisville, KY). Table 1 shows demographic and clinical characteristics of the research participants.

Preoperative MRI recordings

Prior to the implantation surgery, 3D magnetic resonance images from cervical-thoracic (C-T) and thoracic-lumbar (T-L) levels of the spinal cord in axial and sagittal views were recorded (Figs 1A and 2). The images were obtained using a Siemens 3 T Magnetom Skyra (Siemens Medical Solutions) with Turbo Spin Echo and T_2-weighted pulse sequences. Details of MRI acquisition protocol are reported in the Supplementary material.

Intraoperative procedure for spinal cord epidural stimulation paddle placement

During the implantation procedure, anterior-posterior (AP) and lateral fluoroscopy imaging was used to mark the desired vertebral level with the participant in a prone position. A midline bilateral laminotomy was performed, typically at the L1-L2 disc space. The electrode array with 16 contacts (Medtronic Specify® 5-6-5 lead) was advanced into the epidural space via the laminotomy. AP fluoroscopy was used to confirm that the array was as symmetric as possible with respect to the midline. Electrophysiological mapping was performed after initial placement to optimize the positioning of the paddle electrode based on the evoked responses recorded by surface electrodes from soleus, medial gastrocnemius, tibialis anterior, medial hamstrings, vastus lateralis, and rectus femoris (Fig. 1B). Midline local rostral and caudal electrode configurations at 2 Hz, 450 μs were tested to examine the sequence of activation of lower extremity muscles as the stimulation intensity was increased from 0.1 V or 0.5 V with 0.1 V until all muscles reached motor thresholds. The symmetry between left and right sides was evaluated by testing unilateral electrode configurations. If the sequence of muscle activations or the left and right symmetry was not satisfactory, the placement of the electrode array was adjusted, and the mapping process repeated until proper positioning was reached. Following each adjustment of the electrode array, lateral and/or AP fluoroscopy images were taken (Fig. 1B). After final placement was confirmed, the electrode lead was tunnelled subcutaneously and connected to a neurostimulator. Lateral and AP X-ray images were obtained post-operation to record the final placement of the paddle electrode.

Evaluation of number of joints moved post-implant

Participants began the experimental sessions in the laboratory after approximately 2–3 weeks from the surgical implantation of the spinal cord epidural stimulation unit, depending on the

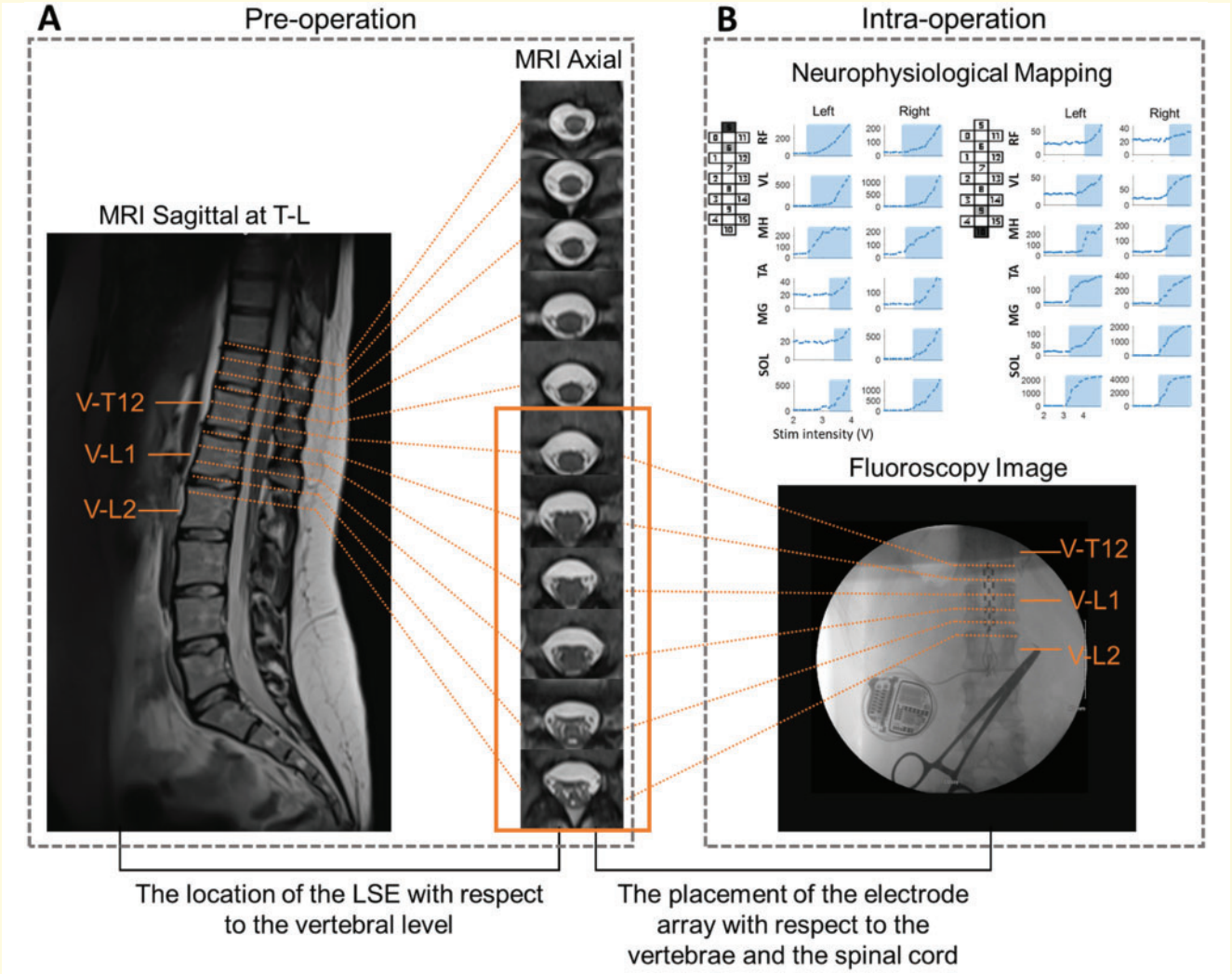

Figure 1 Integration of axial and sagittal MRIs with intraoperative fluoroscopy images to estimate the location of the scES paddle electrode on the spinal cord. (**A**) Example MRIs in sagittal view from the thoracic-lumbar (T-L) level of the spine and corresponding axial MRI slices. (**B**) Neurophysiological mapping of muscle responses to the stimulation at rostral and caudal parts of the array (black contact: cathode/–, grey contact: anode/+) and the corresponding fluoroscopy image indicating the location of the paddle electrode with respect to the bone structure, i.e. vertebral levels. LSE = lumbosacral enlargement; MG = medial gastrocnemius; MH = medial hamstrings; RF = rectus femoris; SOL = soleus; TA = tibialis anterior; VL = vastus lateralis.

time course of wound healing and after clinical clearance was provided by the study neurosurgeon. A series of spatiotemporal mapping experiments in supine position were initially performed. Initial mapping was followed by the selection of scES parameters to facilitate volitional lower limb movements and evaluated by the number of joints moved. All experimental sessions were carried out prior to any training.

Spatiotemporal mapping

The first step post-operation was to perform the spatiotemporal mapping experiments in supine position. During the mapping session, bipolar electrode stimulation using a single adjacent anode and cathode as well as wide field configurations (non-adjacent and multiple anode and cathode combinations) were selected with the pulse width of 450 or 1000 μs. The intensity of the stimulation ramped up stepwise from low to high at low frequency (2 Hz) or high frequency (30 Hz) as well as the frequency ramp up with the intensity fixed at supra threshold. The EMG signals were recorded from 16 leg muscles including right and left gluteus maximus (GL), medial hamstring (MH), rectus femoris, vastus lateralis, tibialis anterior, medial gastrocnemius, soleus, and iliopsoas. The participants did not perform any voluntary movement during the mapping sessions. The outputs of these neurophysiological spatiotemporal mappings would allow identification of the response thresholds and regional responses of each muscle to the stimulation and the segmental location of extensor and flexor muscle groups on the electrode array. These mappings also allowed

identification of the fields that generated rhythmic locomotor activity (Minassian *et al.*, 2004, 2007, 2013; Gerasimenko *et al.*, 2008; Angeli *et al.*, 2018).

Selection of spinal cord epidural stimulation parameters and assessment of volitional movement ability

Lower extremity voluntary movement configurations were then initially estimated using the data obtained from the spatiotemporal mapping sessions. Subsequent assessments in a supine position were performed using the estimated initial configurations while participants attempted voluntary movements (Angeli *et al.*, 2014). Configuration parameters were then optimized during voluntary movements with the goal of achieving the best movement pattern that promoted greatest range of motion. Three different antigravity joint movements were attempted bilaterally (total of six joints). Movements included hallux extension, ankle dorsiflexion and knee to chest flexion. The optimal configuration resulted in stimulation amplitudes that remained submotor threshold when not attempting to move and would promote the best motor output of agonist muscles during attempts. The search of configuration parameters could take 1–5 days and it was performed with and without EMG recording. The number of joints moved (0–6) was determined by the ability to successfully find scES configurations that allowed a minimum of three repetitions of the desired movement under command. This ability was demonstrated prior to any scES training. The performance of voluntary movement experiments was done blinded from the findings of this study. Moreover, the radiographic analysis performed in this study was blinded from the volitional motor outcomes of the research participants.

Radiographic measurements

Spinal cord atrophy and lesion size

Two measurements at the injury site were considered for correlation analysis. The first measurement is the CSA of the spinal cord at the inferior endplate of C3 vertebra that is above the injury site for most of our participants ($n = 19$). Amount of area reduction at this level is an indication of the amount of spinal cord atrophy after SCI (Freund *et al.*, 2013). To calculate this measurement, the area of the spinal cord at this level was manually segmented from the corresponding C-L axial MRI slice (Fig. 2A and B). The segmentation task was performed by two independent trained raters in order to measure the inter-rater variability and ensure that the amount of inter-rater variability does not interfere with the findings.

The second measurement is the length of severe myelomalacia of the cord at the site of injury that was calculated from the C-L axial and sagittal MRI slices for all subjects with proper imaging at the site of injury ($n = 18$) (Fig. 2A and C). This measurement was performed by one trained rater based on counting the number of consecutive axial slices that show severe myelomalacia at the site of injury and the length of severe myelomalacia was calculated by multiplying the number of selected slices by the slice thickness.

Size of the lumbosacral enlargement

To estimate the volume of lumbosacral enlargement above the conus tip, first, we segmented the cord (and the spinal canal) area from the axial MRI slices at the T10-L1 level (Fig. 3A). We then identified the slices with the maximal CSA at the lumbosacral enlargement and the location of the tip of the conus and used these two measurements as reference points. The distance (L) between these two reference points was calculated, and an estimation of the beginning of the enlargement was marked as 2L distance above the conus tip (Fig. 3B). We picked the 2L distance from the conus to ensure the inclusion of the total volume of the lumbosacral in all subjects (Supplementary Fig. 1). Finding the precise beginning of the lumbosacral enlargement is difficult and relatively subjective. The 2L estimation ensures a more consistent and objective measurement across subjects.

Once the estimated beginning of the lumbosacral enlargement is marked, the total volume of the lumbosacral enlargement and conus from the segmented cord CSAs, i.e. the area under the curve in Fig. 3B, was calculated. Finally, a 3D visualization of the lumbosacral enlargement from the segmented MRI slices in coronal view, shown in Fig. 3C, was reconstructed. Since the 'true' maximal CSA at enlargement might be between two consecutive MRI slices, we measured the maximum error range for calculating lumbosacral enlargement volume by going one slice above and one slice below the estimated beginning point of the enlargement and reported the average values and standard deviations. In the 3D visualization, the major diameter of the maximal enlargement was calculated and used as reference for more accurate positioning of the scES paddle electrode on the lumbosacral enlargement.

Spinal cord lumbosacral volume coverage by the electrode array

To estimate the volume of lumbosacral enlargement located under the implanted scES paddle electrode, we integrated the axial and sagittal MRIs with the X-ray images of the final placement of the electrode array. The location of the electrode contacts with respect to the vertebral level is determined using the X-ray, and the amount of cord tissue that is directly covered by the paddle electrode was estimated using axial MRI slices (Fig. 4). To minimize the interference of the angle of the fluoroscopy images in AP view with the accurate assessment of the lumbosacral enlargement coverage, the post-surgery X-ray images in lateral view were mostly used for this measurement. Once the right set of axial slices are selected, the amount of covered cord volume was estimated and the ratio of the lumbosacral enlargement under the paddle to the estimated total volume of the lumbosacral enlargement is reported as a percentage, i.e. estimated percentage of lumbosacral coverage by the scES paddle (Fig. 4C).

The estimated percentage of lumbosacral enlargement volume coverage is consequently related to the positioning of the electrode array with respect to the slices with maximal enlargement and the tip of the conus. Therefore, we also estimated the distance (in millimetres) from the top of the electrode contact at the top of the paddle to the maximal enlargement slice and the distance from the caudal end of the electrode contact at the bottom of the paddle to the tip of the conus. If the paddle is above these two points of reference, the distances were reported as positive values and if below the two reference points, the distances were reported as negative values (Fig. 4C).

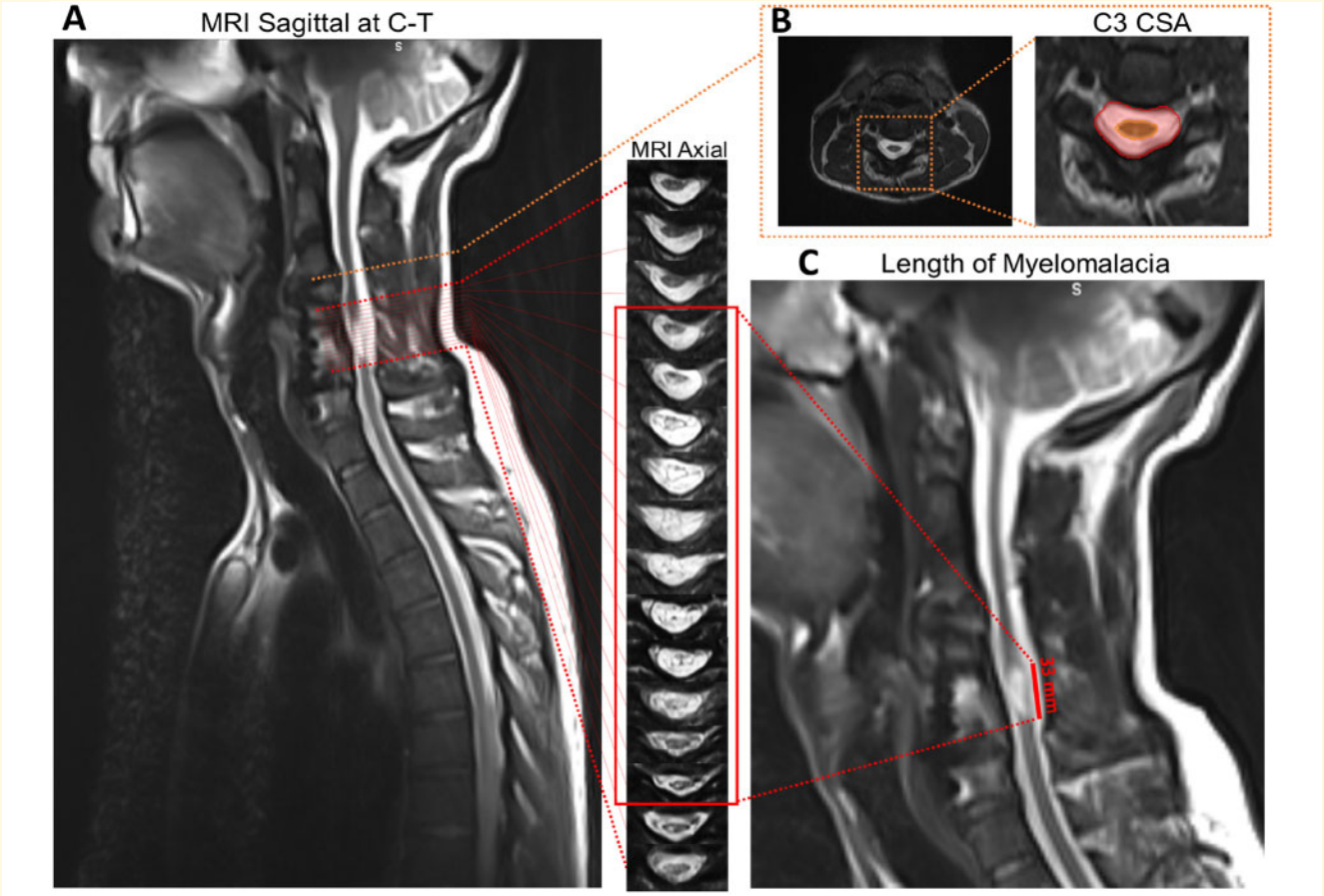

Figure 2 Measurements of the injury site using MRI. (**A**) Example MRI in sagittal view from cervical-thoracic (C-T) level of the spine and the corresponding axial MRI slices. (**B**) CSA of the spinal cord at the inferior endplate of C3 with segmented cord tissue in orange and spinal canal in red. The spinal canal includes both the dura and CSF space within it, and the epidural fat. (**C**) Length of the injury calculated from the axial MRI slices with severe myelomalacia.

Statistical analyses

The statistical significance of correlation values was tested using Pearson's correlation test and P-values < 0.05 considered significant. The Pearson's correlation coefficient (r) values were classified based on the classification table suggested by Hinkle *et al.* (2003). We measured the inter-rater reliability using the intra-class correlation coefficient (ICC) (Ranganathan *et al.*, 2017). To test its significance, we constructed 1000 bootstrap samples to obtain the non-parametric 95% confidence interval built with the 2.5th percentile and 97.5th percentile of the resulting distribution. The ICC values were classified as either poor (<0.5), moderate (0.5–0.75), good (0.75–0.9) or excellent (>0.9) according to the indication proposed by Koo and Li (2016).

All MRI segmentations were done manually using MANGO image processing software (ric.uthscsa.edu/mango). Two blinded independent raters performed all the segmentations. The measurements of CSA and volume of the cord and 3D reconstruction were performed using custom-written codes in MATLAB 2017b. The correlation graphs, linear trend lines, ICC and correlation coefficient values were generated in SAS (SAS Institute Inc.) and Microsoft Excel 2016.

Data availability

All data and algorithms used in this study are included in the manuscript and its Supplementary material or will be available upon request.

Results

The imaging and clinical records of 20 research participants implanted with scES were reviewed in this study. There were 15 males and five females, 14 with AIS A and six with AIS B (Kirshblum *et al.*, 2011). Neurological level of injury ranged from C3 to T4. All individuals were diagnosed as clinically motor complete and the mean duration of injury was 6.4 years ranging from 2.4 to 16.6 years (Table 1).

All individuals achieved voluntary movements after epidural stimulation implantation and prior to any training intervention in the presence of scES. The stimulation parameters, i.e. paddle electrode contacts configuration, intensity, frequency and pulse width, were optimized during voluntary movements for each individual with the goal of achieving

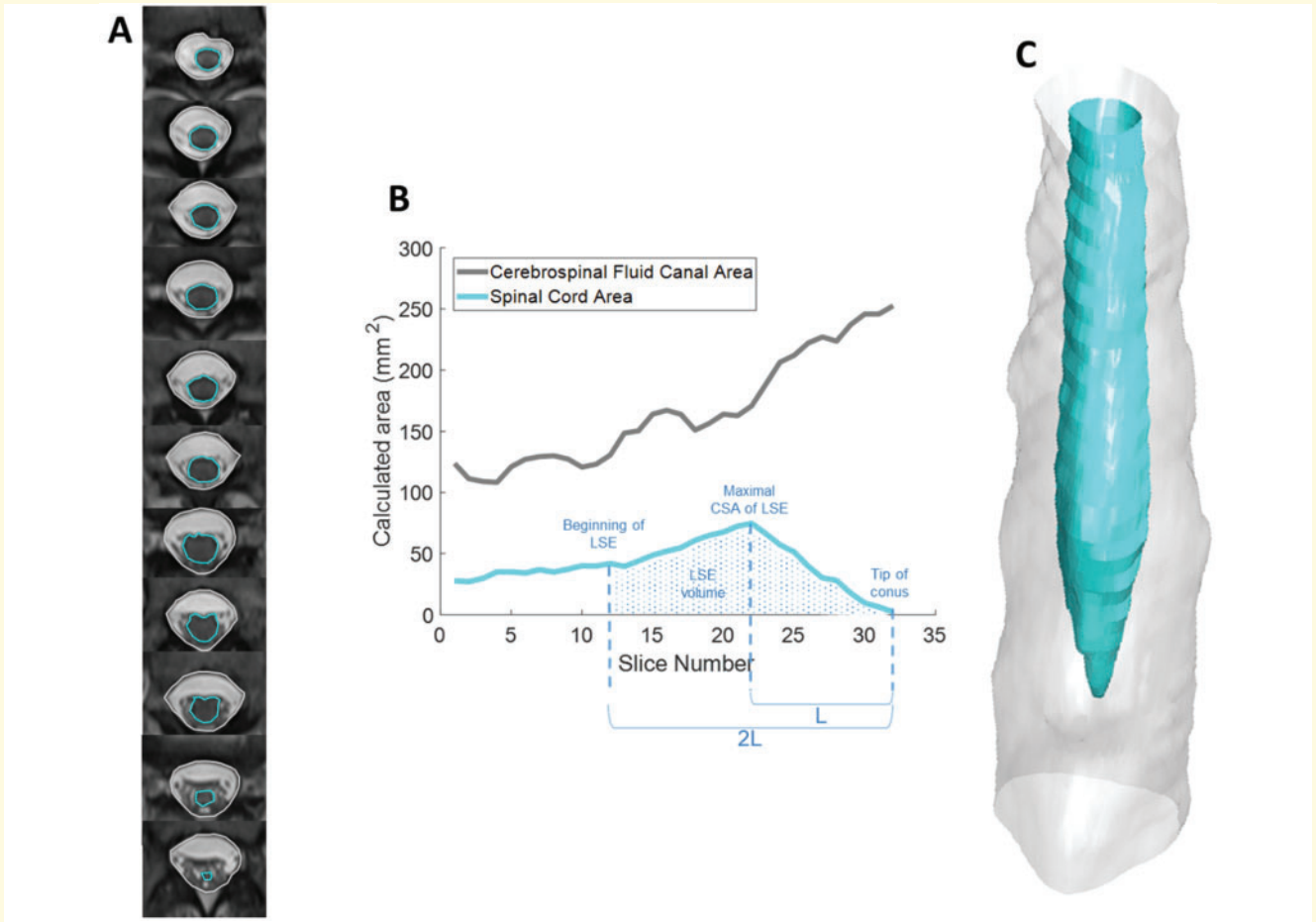

Figure 3 Calculation of the cross-section areas and 3D reconstruction of the spinal cord at lumbosacral enlargement from the axial MRI slices. (**A**) Example MRI slices in axial view with manual segmentation of the spinal cord tissue and the spinal canal highlighted in cyan and grey, respectively. (**B**) CSA of each segmented MRI slice is shown as graphs in cyan for lumbosacral enlargement (LSE) tissue and grey for the spinal canal, the maximal lumbosacral enlargement area, tip of the conus, the distance (L) between the maximal enlargement and conus tip and estimated beginning of the enlargement marked as 2L distance from the conus tip are highlighted with dashed blue vertical lines and the estimated total volume of the enlargement is shown with the blue dotted area. (**C**) Visualization of 3D reconstruction of the spinal cord at lumbosacral enlargement (shown in cyan) from segmented MRI slices and the spinal canal represented in grey.

the best possible movement pattern and maximum number of joints movement. The number of joints (left and right toe, ankle and hip joints, maximum of six) moved for each participant are shown in Table 1.

Figure 5 illustrates the correlation graphs between the calculated radiographic measurements and the lower extremity motor outcomes in the presence of scES. The two measurements of the cord CSA at C3, i.e. above the lesion, ($n = 19$, $r = 0.33$, $P = 0.165$) and the length of severe myelomalacia ($n = 18$, $r = -0.02$, $P = 0.928$) did not significantly correlate with the number of joints moved with scES (Fig. 5A and B). However, the percentage of the cord at lumbosacral enlargement covered by the paddle electrode ($n = 20$, $r = 0.59$, $P = 0.006$) showed a moderate significant correlation with the number of joints moved with scES (Fig. 5C). Moreover, as the percentage of the lumbosacral enlargement coverage is linked to the distance between the paddle electrode and the two points of reference, i.e. maximal lumbosacral enlargement area and tip of the conus, we measured the number of correlations between the sum of these two distances and the volitional responses. As shown in Fig. 5D, the correlation between the sums of distances from the paddle to the maximal enlargement and conus tip ($n = 20$, $r = 0.50$, $P = 0.026$) is also significantly correlated with the number of joints moved. Radiographic measurements for all individuals are reported in Supplementary Tables 1–3.

Because of the uneven distribution of the data around the linear correlation line in Fig. 5C and D, we retested this correlation in the subgroup of research participants (Tanniou *et al.*, 2016) that follow the positive linear trend ($n = 16$), which showed that similar linear correlation still holds but with a much higher correlation coefficient of $r = 0.83$ and $P < 0.0001$ (Supplementary Fig. 2). For the remaining four individuals, the negative trend means that despite having

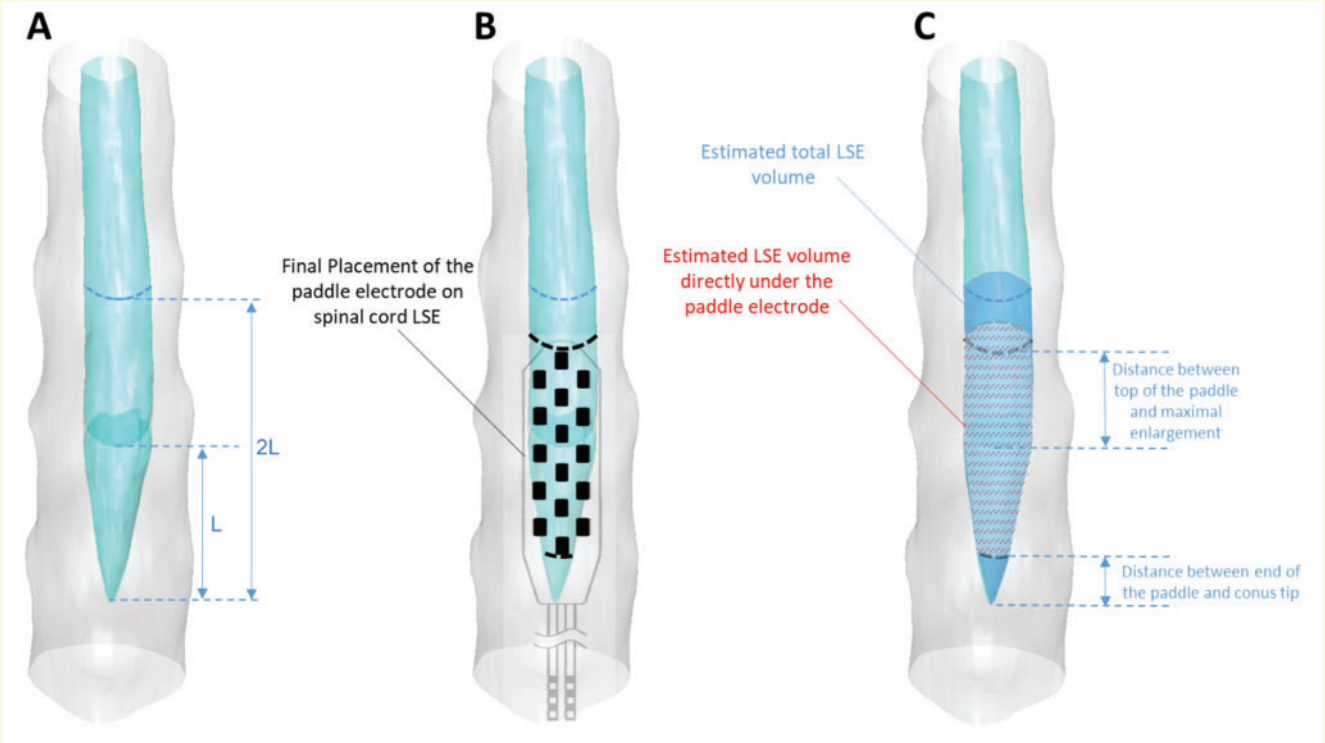

Figure 4 Example **3D reconstructed image of lumbosacral enlargement with paddle electrode placement and visualization of calculated measurements.** (**A**) 3D reconstructed lumbosacral enlargement for Subject A60 with the distance L between the maximal enlargement slice (darker cyan) and conus tip and 2L distance from the conus tip to approximate beginning of the lumbosacral enlargement marked with dashed blue lines. (**B**) Visualization of the final placement of the paddle electrode on the lumbosacral enlargement (LSE) for Subject A60 with an estimated 79% of coverage. The top and end of the paddle electrode are marked with dashed black curves on the cord. (**C**) The estimated total volume of the cord at lumbosacral enlargement is shown with the blue cone and the volume of the cord directly under the paddle is shown with dashed red patterns. The distances between the top of the paddle electrode and the maximal enlargement, and the caudal end of the paddle and the conus tip are shown with dashed blue lines and blue arrows.

relatively fair coverage, they did not move the expected number of joints based on the trend observed in the subgroup: Subject B23 had 40% coverage, which is more than half of the highest per cent coverage reported (79%), but only moved one joint; the same was observed for Subjects A80 and A68 with 53% and 59% coverages, respectively, who only moved one joint; and Subject A77 with 67% coverage, who did not move more than half of their joints.

We also examined the correlations between other demographic and clinical factors such as age, time since injury, maximal enlargement CSA, the estimated total volume of lumbosacral enlargement, and the distance between the maximal enlargement and conus tip, with the number of joints moved voluntarily postoperation and none of these factors showed significant correlations (Supplementary Fig. 3).

To visualize the amount of variability of the electrode array placement among the 20 participants, the results of the volumetric reconstruction of each participant's spinal cord at lumbosacral enlargement with the graphic of the paddle electrode placement over the dura and the acute motor function recovery scores are illustrated in Fig. 6. In these graphs, the width of the paddle electrode and the width of the maximal lumbosacral enlargement slice were considered to represent the electrode positioning better.

The inter-rater reliability was tested for spinal cord CSA above injury and lumbosacral enlargement percentage coverage values and the results showed that the ICC values were 'good' and 'excellent' for these measurements, respectively. Moreover, for both measurements, the difference between the Pearson's correlation coefficients of the two raters were not statistically significant (Supplementary Tables 1 and 3).

Finally, we tested the correlation between the two measurements for paddle placement on lumbosacral enlargement: the percentage of lumbosacral coverage and the positioning of the paddle electrode based on the distances between top of the array and maximal enlargement and bottom of the array and end of conus and showed that these two measures are 'very highly' correlated ($r = 0.90$, $P < 0.0001$, $n = 20$, Supplementary Fig. 4). We also performed sensitivity analysis to compare the Pearson's correlation values of these two paddle placement measurements with the volitional outcomes and found that with $P \leqslant 0.0001$ these two measurements are statistically comparable. This analysis shows that

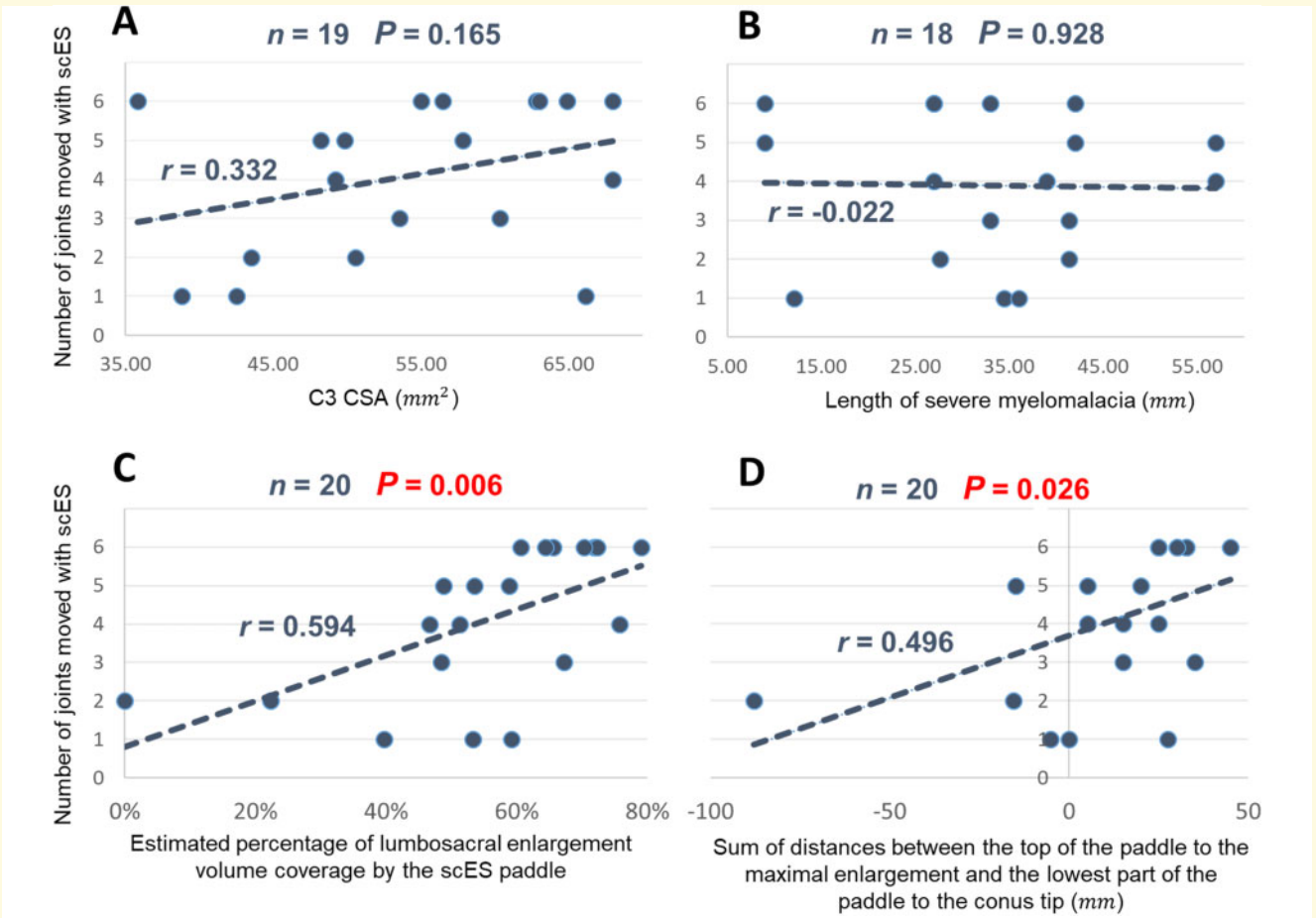

Figure 5 Correlations between the radiographic measurements i.e. the cord CSA at C3 above the injury, length of severe myelomalacia, estimated percentage of lumbosacral enlargement coverage, and the distances from paddle electrode to the maximal enlargement and conus tip, and the number of joints moved with scES. (**A**) Correlation between the CSA of the spinal cord at the inferior endplate of C3 and number of joints moved post-operation for subjects with proper MRI at this level (n = 19). (**B**) Correlation between the length of the severe myelomalacia and number of joints moved post-operation for subjects with proper MRI at this level (n = 18). (**C**) correlation between the percentage of the lumbosacral enlargement volume coverage by the scES paddle electrode and number of joints moved post-operation for all subjects (n = 20). (**D**) Correlation between the sum of distances from the top of the scES paddle to the maximal enlargement the caudal end of the paddle to the conus tip, and number of joints moved post-operation for all subjects (n = 20).

the correlation results found in this study (Fig. 5C and D) are not sensitive to the choice of the measure used. This also assures that the selection of 2L distance as an estimation of the beginning of lumbosacral enlargement adds negligible error to the correlation analysis outcomes.

Discussion

All individuals with chronic and clinically motor complete SCI that participated in the scES study (n = 20) achieved, to some extent, lower extremity voluntary movements post-scES implant and prior to any locomotor, voluntary movement or cardiovascular training. We have shown in this study that the number of joints moved voluntarily post-implant is significantly correlated with the percentage coverage of the spinal cord lumbosacral enlargement by the scES paddle electrode. However, there were no significant correlations between the CSA of the spinal cord above the injury or the length of severe myelomalacia and these motor outcomes. This study is the first to investigate the relationship between volitional joint movements in the presence of scES and the positioning of the stimulation paddle electrode on the lumbosacral enlargement of the spinal cord using MRI and X-ray integration and the 3D volumetric reconstruction of the lumbosacral enlargement. The results of this study suggest that the positioning of the scES paddle electrode to achieve the greatest lumbosacral enlargement coverage would facilitate voluntary recovery of movement in individuals with chronic clinically complete SCI. Moreover, the use of volumetric lumbosacral enlargement reconstruction preoperatively provides a means to optimize placement of epidural stimulators for neuromodulation after SCI.

A second major finding of this study was that amount of severe myelomalacia and cord atrophy above injury did not

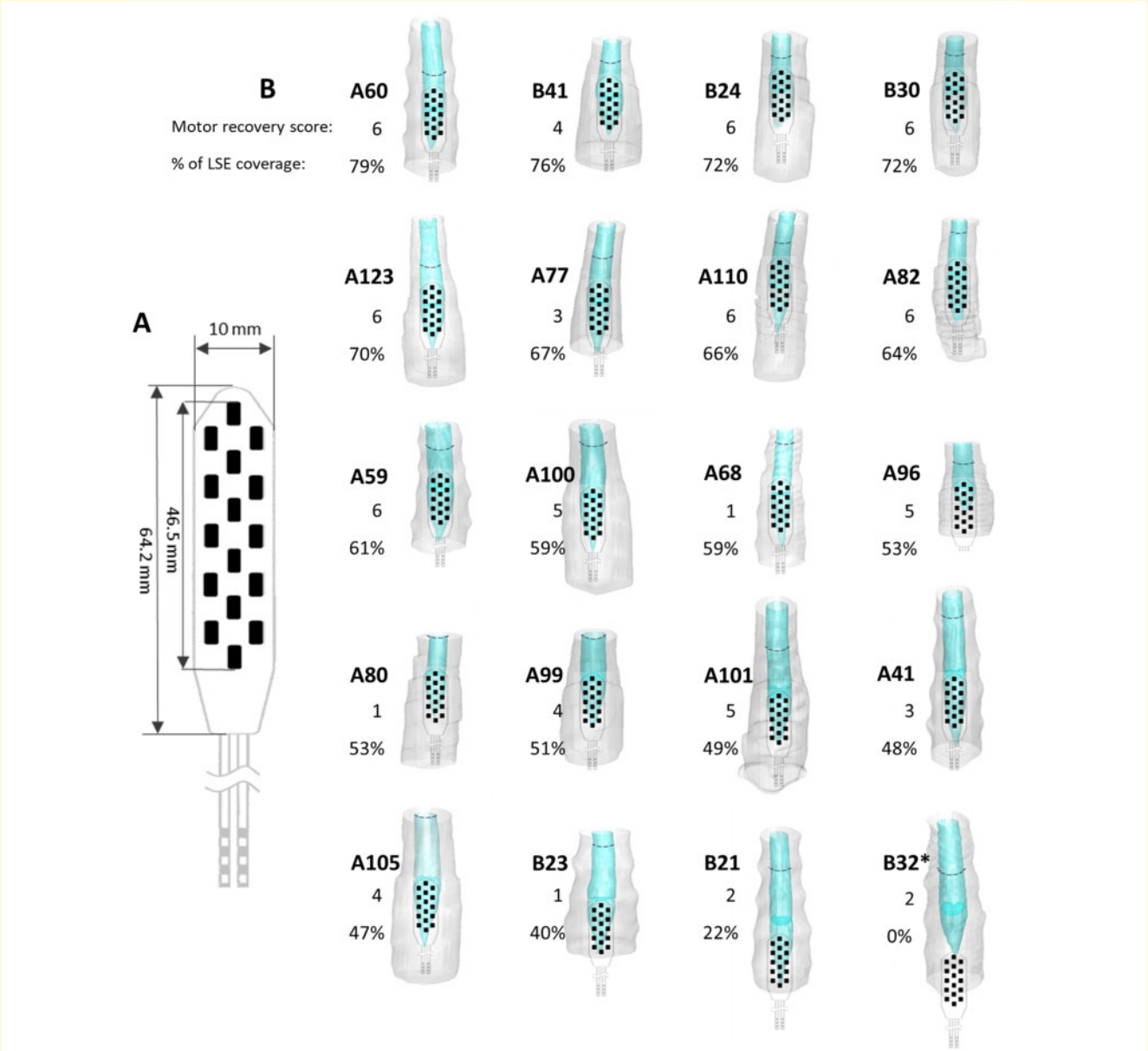

Figure 6 Reconstructed 3D visualization of the spinal cord and relative paddle electrode placement on the lumbosacral enlargement (LSE). (**A**) Dimensions of Medtronic Specify® 5-6-5 lead paddle electrode used for scES, reproduced from Medtronic Manual (permission granted from Medtronic Inc). (**B**) Visualization of reconstructed spinal cords of 20 research participants and the estimated paddle electrode placement with descending order of percentage of lumbosacral enlargement coverage from left to right and up to down. Spinal cord tissue presented in lighter cyan, the spinal canal presented in grey, the epidural stimulation paddle electrode presented in black, the maximal enlargement CSA presented in darker cyan, and 2L distance from the conus tip presented as dark blue dashed curved line. The subject ID, motor recovery score, i.e. number of joints moved voluntarily with scES, and the percentage of lumbosacral enlargement coverage by the paddle electrode is listed next to each graph. *In the case of Subject B32, the best electrophysiological responses were elicited intraoperatively with paddle electrode placed at the caudal aspect of L2, i.e. off the conus.

significantly correlate with the scES motor recovery. Previous studies have reported correlations between the amount of cord atrophy above the injury and extent of sensory and motor functions post-injury in SCI cases when including both motor complete and incomplete SCI (Grabher *et al.*, 2015; Seif *et al.*, 2018). In this study, spinal cord atrophy did not significantly correlate with the functional recovery in the presence of scES when including only those with AIS A and B classifications. This may suggest that the return of lower extremity voluntary function can be achieved with scES in most cases even in the presence of severe post-traumatic radiographic abnormalities.

However, the variability across the research participants regarding the amount of neural tracts at the site of injury or

expansion of the lesion to more distal normal-appearing spinal cord can potentially be contributing factors in regaining volitional recovery (Ellingson *et al.*, 2008; Rutman *et al.*, 2018). Accurate quantification of the amount of residual fibres at the site of injury and measurement of abnormalities in more distal areas may unveil potential links to functional outcomes with scES. Yet, in the few studies that performed diffusion tensor imaging (DTI) and fibre tractography in clinically complete cases, the results of the tractography showed no fibres passing across the injury for AIS A (Chang *et al.*, 2010) while there were significant correlations between the DTI measures and AIS motor scores when including those with clinically incomplete SCI (Ellingson *et al.*, 2008; Cheran *et al.*, 2011).

The observation that all research participants with diagnosed motor complete SCI in this study were able to move their joints voluntarily post-implant may raise the question of whether these imaging methods have proper resolution to accurately detect the limited number of residual pathways that, in the presence of epidural stimulation, transmit the voluntary signal down to the spinal cord circuitry. In chronic and clinically complete SCI cases, quantification of the number of residual neural tracts at the site of injury using fibre tractography is often challenging due to the presence of surgical hardware that causes image artefacts at the injury site (in addition to respiratory and CSF pulsation artefacts). Also the small number of neural sparing that exist in AIS A and B cases can further limit detectability of these structures in the MRI recordings (Rutman *et al.*, 2018).

Functional MRI studies on clinically diagnosed motor complete SCI cases have revealed that in the presence of external motor and sensory stimuli, active dorsal and ventral networks within grey matter above and below the injury site and at lumbar spinal cord were observed even without sensation awareness (Stroman *et al.*, 2004; Kornelsen and Stroman, 2007; Cadotte *et al.*, 2012). Cortical stimulation and recording of evoked muscle responses from paralysed muscles also showed preserved motor pathways as well as existence of voluntary muscle responses in the presence of transcranial magnetic stimulation in most AIS A and B SCI cases studied and two with vestibular pathways observed across the injury level (Squair *et al.*, 2016). The observation that all research participants in this study achieved some voluntary movement provides further evidence that direct neuromodulation of the lumbosacral spinal cord by scES enables the complex spinal networks to access the inputs from previously non-functional and non-detectable residual supraspinal fibres that can mediate intent (Illis, 1995; Bussel *et al.*, 1996; Dimitrijevic *et al.*, 1998; Minassian *et al.*, 2007; Calvert *et al.*, 2019; Rejc and Angeli, 2019). Thus, even after severe SCI, the descending and afferent signals can still reach the intact lumbosacral networks within the spinal cord via the remaining neural pathways; therefore, imaging and neurophysiological assessments need to be further developed and used synergistically for more predictive and mechanistic evaluation of neuroplasticity and recovery as new treatments emerge for SCI.

The achievement of voluntary movements prior to institution of postoperative locomotor training suggests that the findings of this study cannot be explained by Hebbian mechanisms involving combination of scES and postoperative locomotor training (Voronin and Cherubini, 2004; Taccola *et al.*, 2018). Previous studies including finite element modelling of spinal cord tissue structures and distribution patterns of electric field generated by scES suggested that dorsal roots have the lowest activation threshold and are the first structures to activate in the presence of scES (Murg *et al.*, 2000; Rattay *et al.*, 2000; Capogrosso *et al.*, 2013). These studies also suggest that scES can indirectly activate the complex circuitry within the spinal cord through intersynaptic connections with posterior roots. Electrical stimulation of the lumbosacral spinal cord is therefore thought to enable volitional movements by modulating the propriospinal networks that regulate the interpretation of the volitional descending inputs as well as sensory information to generate desired motor patterns (Jankowska *et al.*, 1973; Bui and Brownstone, 2015; James *et al.*, 2018; Taccola *et al.*, 2018). Greater coverage of the lumbosacral enlargement by paddle electrode could mean that most of the propriospinal networks at lumbosacral level can directly be targeted by focused stimulation field at submotor threshold intensities. Additional mechanisms of scES for enabling voluntary movements may include modulation of gene activity and synaptic plasticity at the lumbosacral level (Taccola *et al.*, 2018).

There were no other significant variables observed that correlated with the success of voluntary movement including the time since injury, age, or lumbosacral enlargement volume or CSA. Although significant, the correlation to per cent coverage of the lumbosacral enlargement was moderate and other factors must also contribute to the ability to voluntarily move. Subgroup analyses showed that for 80% of the participants the extent of volitional joint movements is highly correlated with the amount of lumbosacral coverage by the paddle electrode but for the remaining four individuals, there was a negative trend such that despite having relatively fair coverage they did not move more than half of the joints. Paddle electrodes customized to the shape (width and length) of the lumbosacral enlargement in individuals with SCI may lead to better and more consistent performance across participants. The current electrode arrays on the market were designed for treatment of pain and not necessarily for broader SCI neuromodulation. Optimal stimulation configurations may also contribute to the variability. Our approach is to use submotor threshold electrical fields that allow the intentional drive to elicit the voluntary movements. In non-ambulatory, but clinically incomplete individuals with some paralysed muscles, spatiotemporal targeted epidural stimulation above motor threshold based on computational simulations using MRI and CT scans also improved voluntary muscle function (Formento *et al.*, 2018; Wagner *et al.*, 2018). Further study of optimal stimulation for specific SCI populations is warranted and highly likely to be a significant contributor to the success of motor function.

Regardless, the placement of the paddle electrode in relation to the lumbosacral enlargement in all of the studies was of critical importance.

Clinical significance

In the original epidural stimulation study of motor recovery, the research participant reported benefits to the autonomic function in bladder, sexual, and thermoregulatory activity (Harkema *et al.*, 2011). Subsequently epidural stimulation has expanded to many research and clinical sites and the benefits of scES have been reported on motor, bladder, bowel and cardiovascular function in a greater number (Angeli *et al.*, 2014, 2018; Rejc *et al.*, 2015; Grahn *et al.*, 2017; Aslan *et al.*, 2018; Gill *et al.*, 2018; Herrity *et al.*, 2018; Wagner *et al.*, 2018; West *et al.*, 2018; Harkema *et al.*, 2018*a*, *b*; Darrow *et al.*, 2019), but the extent of these benefits varies widely across individuals with SCI. Implementing the methodology used in this study may begin to explain some of this variability. We recommend that other future studies also report the final positioning of the electrode contacts on the array in relation to the lumbosacral enlargement when possible to determine whether the percentage of lumbosacral coverage correlates with motor and non-motor functional outcomes.

Limitations of the study

Although this is the largest case series of scES for neuromodulation in an SCI population to date, the results need to be confirmed in larger multicentre studies to further understand the variability and role of paddle electrode placement. In this study we did not investigate the correlation between the lumbosacral enlargement coverage and the response to standing, stepping, as well as quantification of muscle recruitment patterns and the effects of activity-based recovery training interventions with scES. Additionally, the methods used in this study only measured the atrophy of the spinal cord above the injury site and did not allow direct measurement of the number of residual neurons or neural tracts at the site of injury in these individuals. Future dedicated studies should focus on using more advanced neuroimaging means to perform tractography of supraspinal neural sparing and neural tracts at the site of injury in this most severely injured population and consider synergistic neurophysiological assessments to examine potential links to functional outcomes with scES.

Conclusion

This study establishes that the precise placement of the paddle electrode to ensure maximal coverage of the lumbosacral enlargement is an important consideration for voluntary movement recovery in chronic, clinically diagnosed motor complete SCI. We provide a novel approach using clinically available techniques, fluoroscopy, X-ray, 3D MRI, and intraoperative neurophysiology to optimize scES paddle placement. The optimal design of the paddle electrode and contacts, synergistic imaging and neurophysiology assessments and its effectiveness to achieve the best recovery in SCI population has to be the subject of further investigation.

Acknowledgements

We are indebted to our research participants for their courage, dedication, motivation, and perseverance that made these research findings possible. Glen Hirsch, Darryl Kaelin, Camilo Castillo, Marcus Stoddard and Sarah Wagers provided medical oversight. Yukishia Austin, Lynn Robbins, and Kristen Johnson provided medical management. We would like to thank Dr Yangsheng Chen for engineering leadership and Taylor Blades and Christie Ferreira for project management. Rebekah Morton, Justin Vogt, Katie Pfost, Katelyn Brockman, Brittany Logdson, Ricky Seither, Kristin Benton, Dylan Pfost, and Joseph Carrico lead research interventions and provided support of research participants.

Funding

This work was funded by Christopher and Dana Reeve Foundation (ES-BI-2017), Craig Neilsen Foundation (ES2-CHN-2013), Leona M. & Harry B. Helmsley Charitable Trust (2016PG-MED001), UofL Health - University of Louisville Hospital, Commonwealth of Kentucky Challenge for Excellence Trust Fund and Medtronic Plc. M.B. is supported by the 'Ole A., Mabel Wise and Wilma Wise Nelson Endowed Research Chair'. S.H. is supported by the 'Owsley Brown Frazier Chair in Neurological Rehabilitation'.

Competing interests

The authors report no competing interests.

Supplementary material

Supplementary material is available at *Brain* online.

References

Anderson KD. Targeting recovery: priorities of the spinal cord-injured population. J Neurotrauma 2004; 21: 1371–83.

Angeli CA, Boakye M, Morton RA, Vogt J, Benton K, Chen Y, et al. Recovery of over-ground walking after chronic motor complete spinal cord injury. N Engl J Med 2018; 379: 1244–50.

Angeli CA, Edgerton VR, Gerasimenko YP, Harkema SJ. Altering spinal cord excitability enables voluntary movements after chronic complete paralysis in humans. Brain 2014; 137: 1394–409.

Armour BS, Courtney-Long EA, Fox MH, Fredine H, Cahill A. Prevalence and causes of paralysis-United States, 2013. Am J Public Health 2016; 106: 1855–7.

Aslan SC, Legg Ditterline BE, Park MC, Angeli CA, Rejc E, Chen Y, et al. Epidural spinal cord stimulation of lumbosacral networks modulates arterial blood pressure in individuals with spinal cord injury-induced cardiovascular deficits. Front Physiol 2018; 9: 565.

Bui TV, Brownstone RM. Sensory-evoked perturbations of locomotor activity by sparse sensory input: a computational study. J Neurophysiol 2015; 113: 2824–39.

Bussel B, Roby-Brami A, Rémy Néris O, Yakovleff A. Evidence for a spinal stepping generator in man. Spinal Cord 1996; 34: 91–2.

Cadotte DW, Bosma R, Mikulis D, Nugaeva N, Smith K, Pokrupa R, et al. Plasticity of the injured human spinal cord: insights revealed by spinal cord functional MRI. PLoS One 2012; 7: e45560.

Calvert JS, Grahn PJ, Zhao KD, Lee KH. Emergence of epidural electrical stimulation to facilitate sensorimotor network functionality after spinal cord injury. Neuromodulation 2019; 22: 244–52.

Capogrosso M, Wenger N, Raspopovic S, Musienko P, Beauparlant J, Bassi Luciani L, et al. A. computational model for epidural electrical stimulation of spinal sensorimotor circuits. J Neurosci 2013; 33: 19326–40.

Chang Y, Jung TD, Yoo DS, Hyun JK. Diffusion tensor imaging and fiber tractography of patients with cervical spinal cord injury. J Neurotrauma 2010; 27: 2033–40.

Cheran S, Shanmuganathan K, Zhuo J, Mirvis SE, Aarabi B, Alexander MT, et al. Correlation of MR diffusion tensor imaging parameters with ASIA motor scores in hemorrhagic and nonhemorrhagic acute spinal cord injury. J Neurotrauma 2011; 28: 1881–92.

Darrow D, Balser D, Netoff TI, Krassioukov A, Phillips A, Parr A, et al. Epidural spinal cord stimulation facilitates immediate restoration of dormant motor and autonomic supraspinal pathways after chronic neurologically complete spinal cord injury. J Neurotrauma 2019; 36: 2325–36.

Dimitrijevic MR, Gerasimenko Y, Pinter MM. Evidence for a spinal central pattern generator in humans. Annals NY Acad Sci 1998; 860: 360–76.

Ellingson BM, Ulmer JL, Kurpad SN, Schmit BD. Diffusion tensor MR imaging in chronic spinal cord injury. AJNR Am J Neuroradiol 2008; 29: 1976–82.

Formento E, Minassian K, Wagner F, Mignardot JB, Le Goff-Mignardot CG, Rowald A, et al. Electrical spinal cord stimulation must preserve proprioception to enable locomotion in humans with spinal cord injury. Nat Neurosci 2018; 21: 1728–41.

Freund P, Weiskopf N, Ashburner J, Wolf K, Sutter R, Altmann DR, et al. MRI investigation of the sensorimotor cortex and the corticospinal tract after acute spinal cord injury: a prospective longitudinal study. Lancet Neurol 2013; 12: 873–81.

Gerasimenko Y, Roy RR, Edgerton VR. Epidural stimulation: comparison of the spinal circuits that generate and control locomotion in rats, cats and humans. Exp Neurol 2008; 209: 417–25.

Gill ML, Grahn PJ, Calvert JS, Linde MB, Lavrov IA, Strommen JA, et al. Neuromodulation of lumbosacral spinal networks enables independent stepping after complete paraplegia. Nat Med 2018; 24: 1942.

Grabher P, Callaghan MF, Ashburner J, Weiskopf N, Thompson AJ, Curt A, et al. Tracking sensory system atrophy and outcome prediction in spinal cord injury. Ann Neurol 2015; 78: 751–61.

Grahn PJ, Lavrov IA, Sayenko DG, Van Straaten MG, Gill ML, Strommen JA, et al. Enabling task-specific volitional motor functions via spinal cord neuromodulation in a human with paraplegia. Mayo Clin Proc 2017; 92: 544–54.

Harkema S, Gerasimenko Y, Hodes J, Burdick J, Angeli C, Chen Y, et al. Effect of epidural stimulation of the lumbosacral spinal cord on voluntary movement, standing, and assisted stepping after motor complete paraplegia: a case study. Lancet 2011; 377: 1938–47.

Harkema SJ, Legg Ditterline B, Wang S, Aslan S, Angeli CA, Ovechkin A, et al. Epidural spinal cord stimulation training and sustained recovery of cardiovascular function in individuals with chronic cervical spinal cord injury. JAMA Neurol 2018a; 75: 1569–71.

Harkema SJ, Wang S, Angeli CA, Chen Y, Boakye M, Ugiliweneza B, et al. Normalization of blood pressure with spinal cord epidural stimulation after severe spinal cord injury. Front Hum Neurosci 2018b; 12: 83.

Herrity AN, Williams CS, Angeli CA, Harkema SJ, Hubscher CH. Lumbosacral spinal cord epidural stimulation improves voiding function after human spinal cord injury. Sci Rep 2018; 8: 8688.

Hinkle DE, Wiersma W, Jurs SG, Applied statistics for the behavioral sciences. 5th ed. Boston: Houghton Mifflin; 2003.

Illis LS. Is there a central pattern generator in man? Paraplegia 1995; 33: 239–40.

James ND, McMahon SB, Field-Fote EC, Bradbury EJ. Neuromodulation in the restoration of function after spinal cord injury. Lancet Neurol 2018; 17: 905–17.

Jankowska E, Lundberg A, Stuart D. Propriospinal control of last order interneurones of spinal reflex pathways in the cat. Brain Res 1973; 53: 227–31.

Kirshblum SC, Burns SP, Biering-Sorensen F, Donovan W, Graves DE, Jha A, et al. International standards for neurological classification of spinal cord injury (revised 2011). J Spinal Cord Med 2011; 34: 535–46.

Koo TK, Li MY. A guideline of selecting and reporting intraclass correlation coefficients for reliability research. J Chiropr Med 2016; 15: 155–63.

Kornelsen J, Stroman PW. Detection of the neuronal activity occurring caudal to the site of spinal cord injury that is elicited during lower limb movement tasks. Spinal Cord 2007; 45: 485–90.

McKay WB, Lim HK, Priebe MM, Stokic DS, Sherwood AM. Clinical neurophysiological assessment of residual motor control in post-spinal cord injury paralysis. Neurorehabil Neural Repair 2004; 18: 144–53.

Minassian K, Hofstoetter US, Danner SM, Mayr W, McKay WB, Tansey K, et al. Mechanisms of rhythm generation of the human lumbar spinal cord in response to tonic stimulation without and with step-related sensory feedback. BiomedTech(Berl) 2013; 58 Suppl 1. doi:10.1515/bmt-2013-4013.

Minassian K, Jilge B, Rattay F, Pinter MM, Binder H, Gerstenbrand F, et al. Stepping-like movements in humans with complete spinal cord injury induced by epidural stimulation of the lumbar cord: electromyographic study of compound muscle action potentials. Spinal Cord 2004; 42: 401–16.

Minassian K, Persy I, Rattay F, Pinter MM, Kern H, Dimitrijevic MR. Human lumbar cord circuitries can be activated by extrinsic tonic input to generate locomotor-like activity. Hum Mov Sci 2007; 26: 275–95.

Murg M, Binder H, Dimitrijevic MR. Epidural electric stimulation of posterior structures of the human lumbar spinal cord: 1. muscle twitches - a functional method to define the site of stimulation. Spinal Cord 2000; 38: 394–402.

Ranganathan P, Pramesh CS, Aggarwal R. Common pitfalls in statistical analysis: measures of agreement. Perspect Clin Res 2017; 8: 187–91.

Rattay F, Minassian K, Dimitrijevic MR. Epidural electrical stimulation of posterior structures of the human lumbosacral cord: 2. Quantitative analysis by computer modeling. Spinal Cord 2000; 38: 473–89.

Rejc E, Angeli C, Harkema S. Effects of lumbosacral spinal cord epidural stimulation for standing after chronic complete paralysis in humans. PLoS One 2015; 10: e0133998.

Rejc E, Angeli CA. Spinal cord epidural stimulation for lower limb motor function recovery in individuals with motor complete spinal cord injury. Phys Med Rehabil Clin N Am 2019; 30: 337–54.

Rejc E, Angeli CA, Bryant N, Harkema SJ. Effects of stand and step training with epidural stimulation on motor function for standing in chronic complete paraplegics. J Neurotrauma 2017; 34: 1787–802.

Rutman AM, Peterson DJ, Cohen WA, Mossa-Basha M. Diffusion tensor imaging of the spinal cord: clinical value. Investigational Applications, and Technical Limitations. Curr Probl Diagn Radiol 2018; 47: 257–69.

Seif M, Curt A, Thompson AJ, Grabher P, Weiskopf N, Freund P. Quantitative MRI of rostral spinal cord and brain regions is predictive of functional recovery in acute spinal cord injury. NeuroImage Clin 2018; 20: 556–63.

Sherwood AM, Dimitrijevic MR, McKay WB. Evidence of subclinical brain influence in clinically complete spinal cord injury: discomplete SCI. J Neurol Sci 1992; 110: 90–8.

Squair JW, Bjerkefors A, Inglis JT, Lam T, Carpenter MG. Cortical and vestibular stimulation reveal preserved descending motor pathways in individuals with motor-complete spinal cord injury. J Rehabil Med 2016; 48: 589–96.

Stroman PW, Kornelsen J, Bergman A, Krause V, Ethans K, Malisza KL, et al. Noninvasive assessment of the injured human spinal cord by means of functional magnetic resonance imaging. Spinal Cord 2004; 42: 59–66.

Taccola G, Sayenko D, Gad P, Gerasimenko Y, Edgerton VR. And yet it moves: recovery of volitional control after spinal cord injury. Prog Neurobiol 2018; 160: 64–81.

Tanniou J, van der Tweel I, Teerenstra S, Roes KCB. Subgroup analyses in confirmatory clinical trials: time to be specific about their purposes. BMC Med Res Methodol 2016; 16: 20.

Voronin LL, Cherubini E. 'Deaf, mute and whispering' silent synapses: their role in synaptic plasticity. J Physiol 2004; 557: 3–12.

Wagner FB, Mignardot JB, Le Goff-Mignardot CG, Demesmaeker R, Komi S, Capogrosso M, et al. Targeted neurotechnology restores walking in humans with spinal cord injury. Nature 2018; 563: 65–71.

Waters RL, Yakura JS, Adkins RH, Sie I. Recovery following complete paraplegia. Arch Phys Med Rehabil 1992; 73: 784–9.

Wernig A, Muller S, Nanassy A, Cagol E. Laufband therapy based on 'rules of spinal locomotion' is effective in spinal cord injured persons. Eur J Neurosci 1995; 7: 823–9.

West CR, Phillips AA, Squair JW, Williams AM, Walter M, Lam T, et al. Association of epidural stimulation with cardiovascular function in an individual with spinal cord injury. JAMA Neurol 2018; 75: 630–2.